Mitochondrial Presequence Inserts Differently into Membranes Containing Cardiolipin and Phosphatidylglycerol

Margot M. E. Snel,[‡,§] Anton I. P. M. de Kroon,[||,⊥] and Derek Marsh*[,‡]

Max-Planck-Institut für biophysikalische Chemie, Abteilung Spektroskopie, Postfach 2841, D-37018 Göttingen, Germany, and Department of Chemistry, Stanford University, Stanford, California 94305

Received September 6, 1994; Revised Manuscript Received December 5, 1994[⊗]

ABSTRACT: The interaction of the 25-residue presequence of yeast cytochrome oxidase subunit IV with lipid bilayers composed of phosphatidylglycerol, cardiolipin, or their (1:4) mixtures with phosphatidylcholine has been studied by spin-label ESR spectroscopy. Binding of the presequence progressively broadens the gel-to-fluid phase transition of dimyristoylphosphatidylglycerol bilayers, leading to abolition of the transition at a peptide/lipid ratio of ≥1:5 mol/mol. The mobility of phosphatidylglycerol spin-labeled at the 5-position of the *sn*-2 chain is decreased in both gel and fluid phases on binding the presequence, with a progressively increasing ESR spectral anisotropy in the fluid phase. The ESR spectra of phosphatidylglycerol spin-labeled at the 14-position of the *sn*-2 chain contain a second motionally restricted component, in addition to the fluid bilayer spectral component, that arises from direct interaction of the bound presequence with the lipid chains. The proportion of this motionally restricted component is greater for dioleoylphosphatidylglycerol bilayers (corresponding to 2−3 lipids per peptide) than for cardiolipin bilayers (1−2 lipids/peptide), and this component is present also in the mixed bilayers containing 80% phosphatidylcholine. The ESR spectra of the presequence spin-labeled with a maleimide derivative at cysteine-19 evidence high mobility in solution and a very strong reduction in mobility on binding to bilayers containing negatively charged lipids. At low peptide to lipid ratios, the ESR spectra of the spin-labeled presequence sense the phase transition of dimyristoylphosphatidylglycerol. The membrane location of the spin label on the bound presequence was determined from the paramagnetic relaxation enhancements induced by lipid-permeant molecular oxygen and lipid-impermeant chromium oxalate by using calibrations established with spin-labeled lipids in the presence of presequence alkylated with *N*-ethylmaleimide. The label on cysteine-19 is positioned between the 5- and 14-positions of the lipid chain when bound to dioleoylphosphatidylglycerol and in the region of the 14-position for (1:4) admixture with phosphatidylcholine. When bound to cardiolipin bilayers, the location is shifted toward the membrane surface: to the headgroup region for cardiolipin alone and to the 5-position of the chain for (1:4) admixture with phosphatidylcholine. Possible functional consequences of the different localization of the presequence in phosphatidylglycerol and cardiolipin membranes are discussed.

Presequences are N-terminal extensions of mitochondrial precursor proteins that are synthesized in the cytosol. They contain the information to target the precursors to their final destination in the mitochondrion. Upon import into the mitochondria, the presequences are removed proteolytically to yield the mature proteins. The amino acid sequences of presequences destined for the same mitochondrial compartment show little homology. Presequences that direct precursor proteins to the mitochondrial matrix are generally enriched in positively charged, hydroxylated, and apolar amino acid residues (Von Heijne, 1986). After binding to a presequence receptor at the outer mitochondrial membrane, the precursors are transported across one or two membranes mediated by the proteinaceous mitochondrial translocation machinery, via a so far unknown molecular mechanism. Translocation of the presequence across the inner mitochondrial membrane requires a transmembrane electrical potential. It has been proposed that protein translocation occurs through dynamic contact sites between the outer and inner mitochondrial membranes [for a recent review on mitochondrial protein import, see Kiebler et al. (1993)].

Several synthetic presequences have been shown to interact with phospholipid membranes (Tamm, 1991), suggesting a possible role for the membrane lipids in the import process. The synthetic 25-residue presequence of yeast cytochrome oxidase subunit IV (p25)[1] has been the subject of various

* To whom correspondence should be addressed.

‡ Max-Planck-Institut.

§ Present address: Leiden Institute of Chemistry, Gorlaeus Laboratories, Leiden University, The Netherlands.

|| Stanford University.

⊥ Present address: Centre for Biomembranes and Lipid Enzymology, Department of Biochemistry of Membranes, Utrecht University, The Netherlands.

⊗ Abstract published in *Advance ACS Abstracts,* March 1, 1995.

[1] Abbreviations: p25, 25-residue presequence of yeast cytochrome oxidase subunit IV of sequence MLSLRQSIRFFKPATRTLCSSRYLL-$CONH_2$; ESR, electron spin resonance; CW, continuous wave; CL, cardiolipin (diphosphatidylglycerol); DOPG, 1,2-dioleoyl-*sn*-glycero-3-phosphoglycerol; DOPC, 1,2-dioleoyl-*sn*-glycero-3-phosphocholine; DMPG, 1,2-dimyristoyl-*sn*-glycero-3-phosphoglycerol; DMPC, 1,2-dimyristoyl-*sn*-glycero-3-phosphocholine; *n*-PGSL, 1-acyl-2-[*n*-(4,4-dimethyloxazolidine-*N*-oxyl)stearoyl]-*sn*-glycero-3-phosphoglycerol; T-PASL, 4-phosphatidyl-2,2,6,6-tetramethylpiperidine-1-oxyl; NEM, *N*-ethylmaleimide; 5-MSL, 3-maleimido-2,2,5,5-tetramethylpyrrolidine-*N*-oxyl; p25-MSL, p25 presequence spin-labeled at cysteine-19 with 5-MSL; p25-NEM, p25 presequence alkylated at cysteine-19 with NEM; CROX, potassium tris(oxalato)chromate(III) trihydrate; Hepes, *N*-(2-hydroxyethyl)piperazine-*N*′-2-ethanesulfonic acid; EDTA, (ethylenedinitrilo)tetraacetic acid; L/P, molar lipid to peptide ratio.

0006-2960/95/0434-3605$09.00/0

biophysical studies on these membrane interactions. Negatively charged lipids strongly enhance the interaction of p25 with membranes (Roise et al., 1986; Tamm, 1986; Frey & Tamm, 1990). p25 adopts an amphipathic, partially α-helical structure in detergent micelles (Roise et al., 1986) and in negatively charged phospholipid bilayers (Tamm & Bartoldus, 1990). The α-helix is located in the N-terminal half of p25 (residues 3−11; Endo et al., 1989). Fluorescently labeled p25, with the fluorophore at cysteine-19, was shown to be imported into isolated yeast mitochondria in a process that involves an initial association of p25 with the lipid bilayer (Roise, 1992). Recently, it was shown that p25 is able to induce intermembrane contacts between vesicles (Leenhouts et al., 1993) and between a lipid monolayer and vesicles (Török et al., 1994) with a remarkable specificity for the unique mitochondrial lipid cardiolipin. Vesicle−vesicle contacts could be dissociated when an electrical potential was generated across the bilayers, suggesting that p25 is electrophoretically moved into or even across the bilayer (De Kroon et al., 1991; Maduke & Roise, 1993).

In the present study, the membrane interactions and location of p25 are determined by spin-label ESR spectroscopy. The membranes contained either cardiolipin (CL) or phosphatidylglycerol (PG) as the negatively charged lipid component. CL was selected because it is the most abundant acidic lipid in mitochondria (Daum, 1985) and because of the proposed specific p25-CL interaction (see above). Comparison is made to PG that was chosen to represent the other acidic phospholipids. First, the ability of p25 to restrict the mobility of phospholipids, spin-labeled at the 5- or 14-position in the *sn*-2 chain, was studied in lipid membranes consisting of dimyristoyl- and dioleoylphosphatidylglycerol (DMPG and DOPG, respectively), CL, and mixtures of DOPG and CL with dioleoylphosphatidylcholine (DOPC). This ESR method indicated indirectly the localization of p25 within the membrane. Second, the spatial membrane location of p25 was determined directly by CW saturation ESR spectroscopy. This method is based on the exposure of the nitroxide spin label to paramagnetic relaxation agents that are soluble either in the hydrophobic membrane interior (molecular oxygen) or in the aqueous phase (chromium oxalate). Changes in the nitroxide relaxation times due to interactions with the faster relaxing paramagnetic species are a measure of their accessibility to the nitroxide group [see e.g., Snel and Marsh (1993) and Snel et al. (1994b)]. For this purpose, p25 was spin-labeled at the unique cysteine (residue-19), and its location in a membrane environment consisting of CL and DOPG alone or mixed with DOPC was determined by studying the accessibility to oxygen and chromium oxalate.

EXPERIMENTAL PROCEDURES

Materials. DMPG was synthesized from DMPC (Fluka, Buchs, Switzerland) according to the method of Comfurius and Zwaal (1977). DOPG and DOPC were obtained from Avanti Polar Lipids (Birmingham, AL), and beef heart CL was obtained from Sigma Chemical Co. (St. Louis, MO). Phosphatidylglycerols spin-labeled either at the 5- or at the 14-position in the *sn*-2 chain (5- and 14-PGSL, respectively, where *n*-PGSL is 1-acyl-2-[*n*-(4,4-dimethyl-oxazolidine-*N*-oxyl)stearoyl]-*sn*-glycero-3-phosphoglycerol), were synthesized by B. Angerstein, as described in Marsh and Watts (1982). Phosphatidic acid spin-labeled at the phosphate of the lipid headgroup (T-PASL, 4-phosphatidyl-2,2,6,6-tetramethylpiperidine-1-oxyl) was prepared by H. Eibl and A. Watts at this institute, according to the method of Eibl (1978). Potassium tris(oxalato)chromate(III)trihydrate (CROX) was synthesized as described by Bailar and Jones (1939) and characterized as described by Malati and Abdul Azim (1959, 1960). The peptide corresponding to the presequence of cytochrome oxidase subunit IV, p25 (H_3N^+-Met-Leu-Ser-Leu-Arg-Gln-Ser-Ile-Arg-Phe-Phe-Lys-Pro-Ala-Thr-Arg-Thr-Leu-Cys-Ser-Ser-Arg-Tyr-Leu-Leu-$CONH_2$), was synthesized on an Applied Biosystems 431A peptide synthesizer (Foster City, CA) and purified as described in De Kroon and McConnell (1994).

Labeling of p25. Spin-labeled p25 was prepared by reacting the single cysteine residue at sequence position 19 with 3-maleimido-2,2,5,5-tetramethyl-pyrrolidine-*N*-oxyl (5-MSL, Aldrich, Milwaukee, WI). Typically, 1 μmol of p25 was dissolved in 0.1 M ammonium acetate, pH 8.1, to give a 4.8 mg/mL solution. Any oxidized cysteine residues were reduced with 0.5 μmol of dithiothreitol by reaction for 30 min at room temperature. To this mixture, 6 μmol of 5-MSL was added from a 0.25 M ethanolic 5-MSL solution (3-fold excess over total sulfhydryl groups). The mixture was incubated for 1.5 h at room temperature. The progress of the reduction and spin-labeling reaction was followed by injecting aliquots of the reaction mixture on an analytical C_{18} reverse-phase HPLC column, eluted with water−acetonitrile gradients in 0.1% (v/v) trifluoroacetic acid. The spin-labeled p25 (p25-MSL) was purified from the reaction mixture by HPLC as described above. To prevent the formation of any disulfide-bridged dimers of p25 in the non-spin-labeled p25 experiments, p25 was reacted with *N*-ethylmaleimide (NEM) according to the method given above. Peptide recovery was 60−70% and the purity of p25-MSL and p25-NEM ≥95%. p25 stock solutions in 10 mM Hepes, 50 mM NaCl, and 0.1 mM EDTA, pH 7.0 (1−5 mg/mL) were stored in aliquots at −30 °C.

ESR Sample Preparation. For preparation of lipid dispersions, a dry lipid film was prepared from 0.2−0.25 mg of the desired lipid (mixture) and 1 mol % spin-labeled lipid, with 0.1 mol % butylated hydroxytoluene to prevent lipid peroxidation. This was then hydrated with 10−12.5 μL of buffer (10 mM Hepes, 50 mM NaCl, 0.1 mM EDTA, pH 7.0). When required, the appropriate volume of 4.7 mg/mL p25-NEM (or of 3.7 mg/mL p25-MSL) solution in buffer was added. After incubation at 37 °C for 30 min, the samples were transferred to 1-mm i.d. ESR capillaries and concentrated by centrifugation (1000*g*, 10 min). In a typical experiment, 0.2 mg of DMPG + 5-PGSL was hydrated with 10 μL of buffer, and 40.4 μL of 4.7 mg/mL p25-NEM solution was added (i.e., L/P added = 5 mol/mol; finally determined L/P = 5 mol/mol).

For preparation of lipid-p25 (-MSL or -NEM) samples used in the CW saturation experiments, 30.5 μL of a 1.45 mg/mL p-25 solution was added to 0.25 mg of lipid hydrated with 12.5 μL of buffer. The samples subsequently were incubated at 37 °C for 30 min, and the resulting p25−lipid complexes were collected by centrifugation (8000*g*, 10 min). The pellets were then washed and resuspended in 30 μL of buffer, when required in 10 mM CROX freshly dissolved in argonated buffer. Subsequently, the samples were transferred to capillaries and concentrated further by centrifugation, after which the supernatant was replaced by fresh buffer.

With the exception of cardiolipin alone, all samples precipitated on adding the peptide, either immediately or on incubation. All samples with added peptide could be pelleted on centrifugation. No evidence was found for micelle formation induced by the peptide. The observations also indicate that the lipid−peptide complexes had reached equilibrium on incubation (cf. Leenhouts et al., 1993).

For experiments in the presence or absence of oxygen, buffers were saturated either with oxygen or with argon, and sample tubes and ESR capillaries were flushed with oxygen or argon, respectively. Excess supernatant and sample were removed from the pellets in the ESR capillaries to obtain samples ≤5 mm in length, so as to avoid inhomogeneities of the microwave and modulation fields in the ESR cavity (cf. Fajer & Marsh, 1982).

After the ESR measurements, the lipid to peptide ratios (L/P) of the lipid−p25 complexes were determined. The phospholipid concentration was assayed by the method of Rouser et al. (1970), and the p25 content was determined by the bicinchoninic acid assay (Pierce, Rockford, IL), with bovine serum albumin as standard. Concentrations of CL are always expressed on a phosphorus basis.

ESR Spectroscopy. ESR measurements were performed on a Varian E-12 Century Line 9 GHz ESR spectrometer. Sample capillaries were centered in a standard 4 mm quartz tube containing light silicone oil for thermal stability; temperature was regulated with a pure nitrogen gas-flow system. ESR spectra were recorded with a modulation frequency of 100 kHz and a modulation amplitude of 1.25 Gauss peak-to-peak. The total scan width was 100 Gauss. CW saturation experiments were performed as described by Snel and Marsh (1993), with instrumental calibrations and data analysis as given in the same reference.

RESULTS

Conventional ESR Spectroscopy of Spin-Labeled Presequence and Spin-Labeled Lipids. The ESR spectra of the spin-labeled p25 presequence in solution and bound to DMPG lipid dispersions are shown in Figure 1, spectra A and B, respectively. Clearly, a large reduction in mobility of the spin label takes place on binding of p25 to negatively charged lipid membranes. The spectrum of p25-MSL in the presence of lipid (Figure 1B) consists of a broad, immobile component, characterized by an outer hyperfine splitting of 57 Gauss, with a small narrower, mobile component superimposed. Subtraction of the spectrum of spin-labeled p25 in buffer (Figure 1A) from the spectrum of the lipid-bound p25 (Figure 1B) removes the mobile component (1−2% of the total spectral intensity), demonstrating that this small mobile component represents unbound p25-MSL. The ESR spectra of the 5-PGSL phosphatidylglycerol spin label incorporated in DMPG in the presence and absence of alkylated presequence (p25-NEM) are given in Figure 1C. In the presence of p25-NEM, the 5-PGSL exhibits a larger outer hyperfine splitting (57 Gauss) than in the absence of p25-NEM (50 Gauss), demonstrating a considerable reduction in mobility of the acyl chains of the lipid on binding the presequence.

Figure 2A shows the temperature dependence of the outer hyperfine splitting ($2A_{max}$) of the 5-PGSL spin label incorporated in DMPG membranes in the absence and presence of various amounts of the p25 presequence. The gel-to-liquid-crystalline phase transition of the phospholipid is accompanied by a significant increase in lipid chain mobility. The outer hyperfine splitting of 5-PGSL is a sensitive parameter for this increase in mobility. The phase transition of DMPG is indicated by a steep decrease of $2A_{max}$ in the temperature range of 22−24 °C, which corresponds with the transition temperature of 23 °C for DMPG bilayers in the charged state (Watts et al., 1978; Van Dijck et al., 1978). Increasing binding of the presequence progressively broadens the chain-melting transition of the lipid (L/P ratios of 27 and 11 mol/mol). At higher peptide concentrations, the lipid phase transition is abolished completely (L/P ratios of 3 and 5 mol/mol). In addition, Figure 2A shows that below and above the phase transition of DMPG the values of $2A_{max}$ in all lipid−p25 complexes are larger than those of the lipid alone. This means that the lipid spin label mobility both in the gel phase and in the fluid phase is restricted by binding of p25. In the fluid phase, this restriction of the lipid mobility increases progressively with the amount of presequence that is bound.

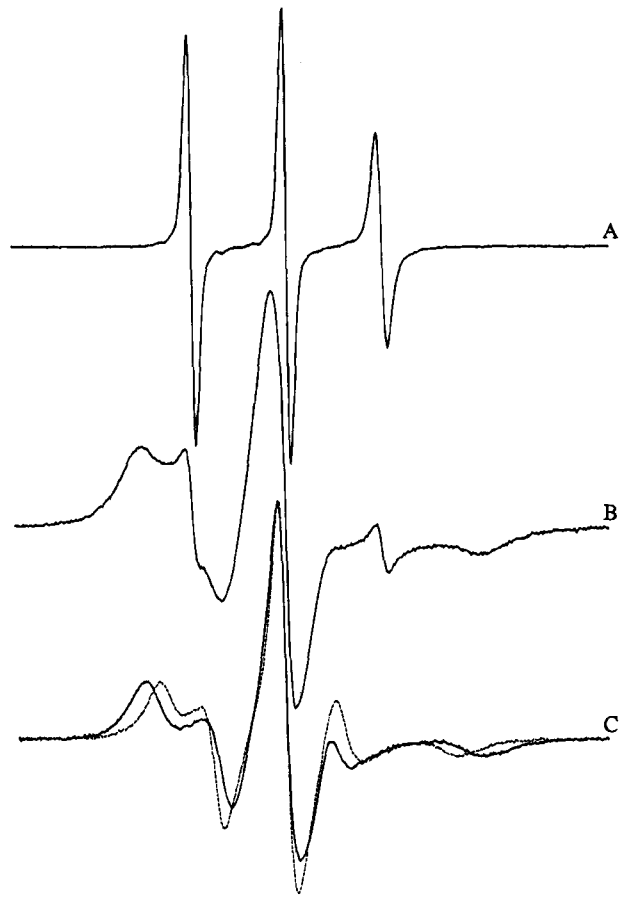

FIGURE 1: ESR spectra recorded at 30 °C of (A) 0.45 mM p25-MSL in buffer, (B) p25-MSL bound to DMPG at L/P = 29 mol/mol, and (C) 5-PGSL incorporated in DMPG, (dashed line) lipid alone, (solid line) with p25-NEM bound at L/P = 5 mol/mol. Total scan width = 100 Gauss.

Figure 2B shows the temperature dependence of $2A_{max}$ for spin-labeled p25 bound to DMPG at various L/P ratios. At L/P = 29 mol/mol, the spin label on the peptide senses the phase transition of the lipid. This might indicate that the spin label on p25 is located within the hydrophobic part of the membrane and that the presequence is integrated to some extent within the bulk lipid matrix. (That a spin label on a peripherally bound peptide senses the phase transition or it

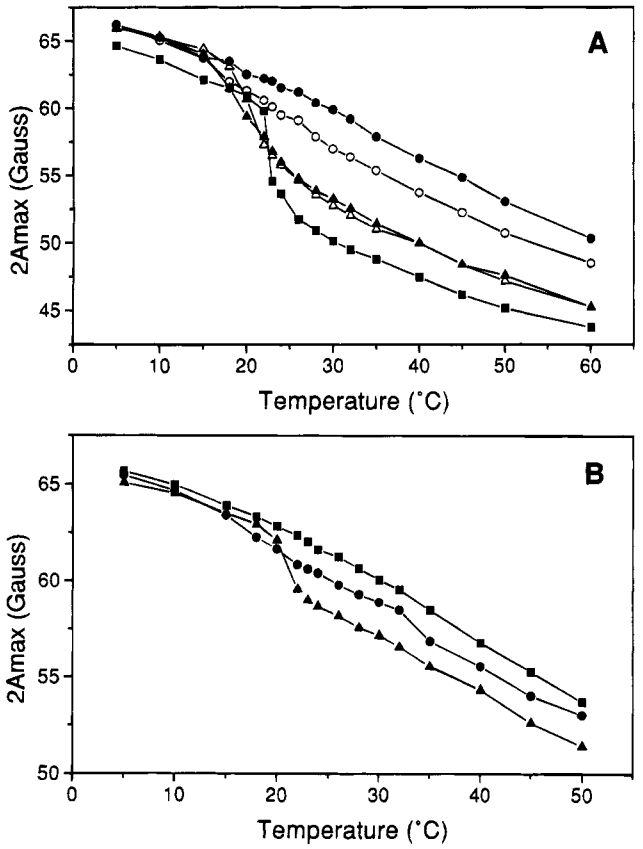

FIGURE 2: Temperature dependence of the outer hyperfine splitting ($2A_{max}$) of (A) 5-PGSL incorporated in DMPG-p25-NEM complexes, (■) lipid alone, and complexes of final L/P: (△) 27 mol/mol (27 mol/mol added), (▲) 11 mol/mol (12 mol/mol added), (○) 5 mol/mol (5 mol/mol added), and (●) 3 mol/mol (4 mol/mol added); and (B) p25-MSL bound to DMPG at L/P (▲) 29 mol/mol (26 mol/mol added), (●) 10 mol/mol (10 mol/mol added), and (■) 5 mol/mol (5 mol/mol added).

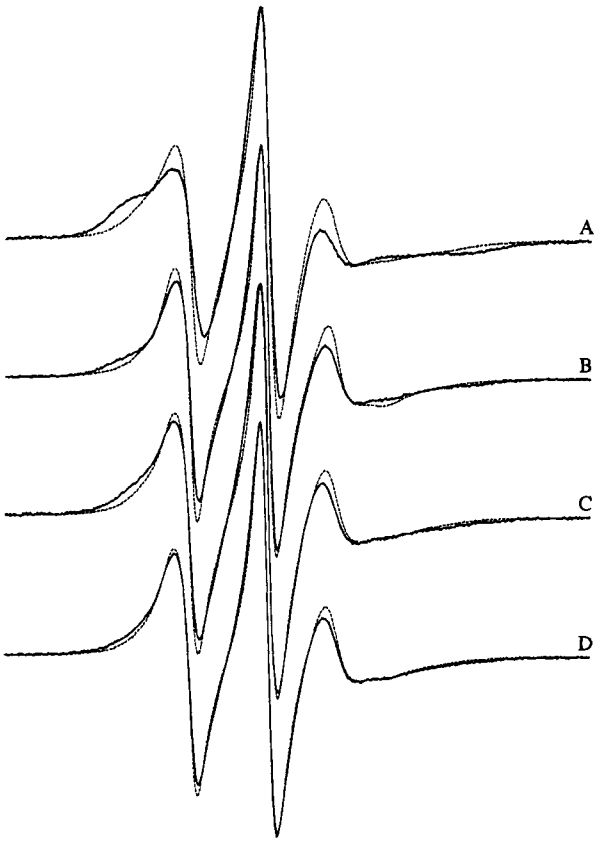

FIGURE 3: ESR spectra of 14-PGSL incorporated in various lipid membranes in the presence (solid lines) and absence (dashed lines) of p25-NEM, recorded at 5 °C. (A) DOPG, L/P 7.4 mol/mol; (B) CL, L/P 6.8 mol/mol; (C) DOPG/DOPC = 1:4 mol/mol, L/P 7.8 mol/mol; (D) CL/DOPC = 1:4 mol/mol, L/P 9.0 mol/mol. In each case, peptide was added at an initial L/P of 6 mol/mol. Total scan width = 100 Gauss.

alone penetrates into the bilayer seems less likely, although this cannot be excluded entirely.) When higher amounts of p25 are bound to DMPG, the lipid transition sensed by the spin-labeled presequence is very much broadened (L/P 10 mol/mol) or wiped out completely (L/P 5 mol/mol), in agreement with the results obtained with the spin-labeled lipid in Figure 2A.

The ESR spectra of phosphatidylglycerol spin-labeled at the 14-position of the chain (14-PGSL) and incorporated in negatively charged lipid membranes of different compositions, both in the presence and in the absence of p25-NEM, are given in Figure 3. In the presence of p25-NEM, all spectra are broadened, especially in the outer wings. In particular, the spectra from membranes composed of DOPG and CL alone clearly are two-component in nature. The component seen in the outer wings of the spectra is motionally restricted by p25-NEM and represents the fraction of lipids directly in contact with it. The other component corresponds to fluid lipids that are in slow exchange with the peptide-associated lipids on the conventional nitroxide ESR time scale. These have a spectral line shape similar to that of the lipids alone, although with somewhat increased line broadening and spectral anisotropy. The slow exchange leads only to a slight broadening of this fluid component (Horváth et al., 1988; cf. dashed lines in Figure 3). The second, motionally restricted spectral component is less clear in the spectra from the samples containing zwitterionic lipid which presumably indicates a different mode of lipid–peptide interaction in these samples. Similarly, the relative line heights of the motionally restricted component decrease with increasing temperature because of the steeper temperature dependence of the fluid component line shapes (data not shown). The relative proportions of the individual components in the two-component spectra were quantitated by spectral subtractions as described earlier (Marsh, 1982). Briefly, the method involves subtracting a fluid lipid spectrum obtained for the spin label in pure lipid bilayers (cf. dashed lines in Figure 3) from the spectrum of the lipid–p25 complexes (cf. solid lines in Figure 3). The difference spectrum represents the motionally restricted spin-labeled lipid component. To determine the endpoint of the subtraction, the spectrum of the immobilized component was matched to a motionally restricted spectrum of the 14-PCSL spin label incorporated in dimyristoylphosphatidylcholine sonicated vesicles in the gel state. Subtractions performed in the reverse direction confirmed the fractions obtained for the motionally restricted component in the lipid–p25 complexes. The results of the spectral subtractions are given in Table 1. It will be noted that, in the mixtures of the two negatively charged lipids with phosphatidylcholine, there is little selectivity between these two lipids in their competition with the spin-labeled lipid for interaction with the peptide. Therefore, the considerable differences in the degree of association of the spin-labeled lipid with the peptide in complexes with the negatively charged lipids alone (at two

Table 1: Fractions (f) of the Motionally Restricted 14-PGSL Spin Label in Different Lipid−p25-NEM Complexes at the Lipid to Peptide Ratio (L/P) and Temperature (T) Indicated[a]

	L/P (mol/mol)	T (°C)	f
DOPG	7.4	10	0.40
		15	0.34
		20	0.32
DOPG	10.5	10	0.27
		15	0.23
		20	0.19
DOPG/DOPC (1:4 mol/mol)	7.8	10	0.24
		15	0.26
CL	6.8	10	0.20
		15	0.22
		20	0.21
CL	10.2	10	0.06
		15	0.09
		20	0.05
CL/DOPC (1:4 mol/mol)	9.0	10	0.26
		15	0.24

[a] In all cases (i.e., including CL), L/P is referred to moles of lipid phosphate.

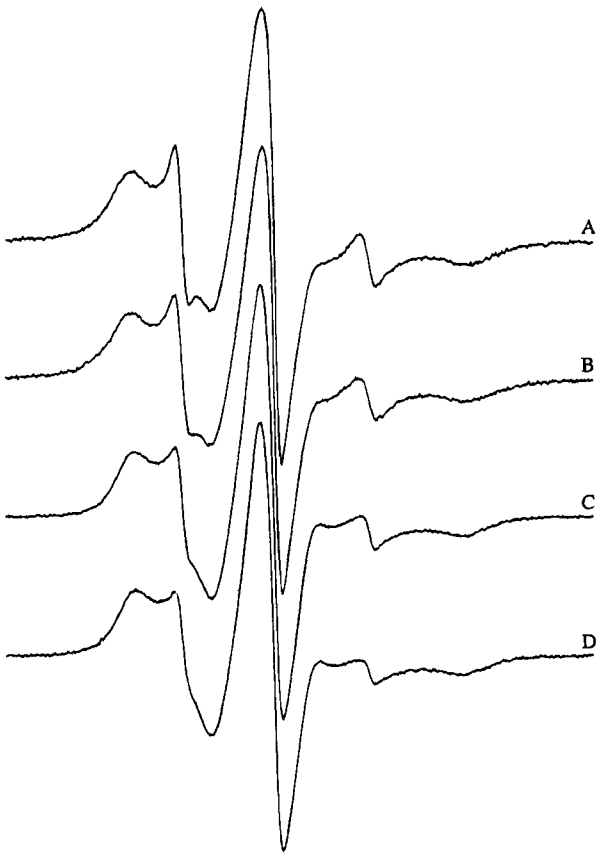

FIGURE 4: ESR spectra of p25-MSL bound to various lipid membranes, recorded at 30 °C. (A) DOPG, L/P 32 mol/mol; (B) CL, L/P 24 mol/mol; (C) DOPG/DOPC = 1:4 mol/mol, L/P 26 mol/mol; (D) CL/DOPC = 1:4 mol/mol, L/P 33 mol/mol. In each case, peptide was added at an initial L/P of 23 mol/mol. Total scan width = 100 Gauss.

different L/P ratios) is attributable to differences in the stoichiometry of association.

The ESR spectra of spin-labeled p25 bound to DOPG, CL, and their 1:4 mol/mol admixtures with DOPC are given in Figure 4. In all cases, the major portion of the spin label is immobilized on binding of p25 to the various membranes (cf. Figure 1A). The immobile component in the spectra at 30 °C is characterized by an outer hyperfine splitting of 57.4

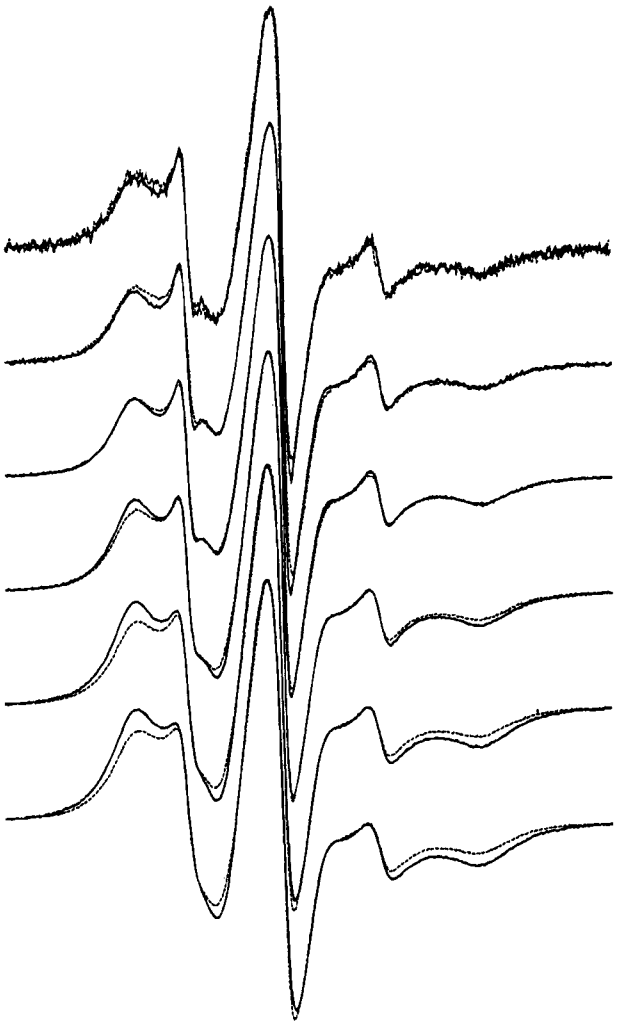

FIGURE 5: ESR spectra of p25-MSL bound to DOPG membranes, at L/P 32 mol/mol in the absence (solid lines) and in the presence (dashed lines) of oxygen, recorded at 30 °C. From top to bottom the microwave power at which the spectra are recorded is increasing, corresponding to values of $\langle H_1^2\rangle^{1/2} \approx$ 19, 57, 173, 300, 418, and 522 mGauss. Spectra are normalized to the same central line height. Peptide was added at an initial L/P of 23 mol/mol. Total scan width = 100 Gauss.

(A), 57.3 (B), 56.3 (C), and 55.8 (D) Gauss. In comparison with outer hyperfine splittings observed for 5-MSL spin-labeled integral membrane proteins such as the sodium/potassium ATPase (66.5−67.5 Gauss at 0 °C; Esmann et al., 1989), the values obtained for membrane bound p25 are unexpectedly high for a 25-residue amphipathic peptide. This indicates that p25 is intimately associated with the (mixed) phospholipid membranes and suggests that the interaction is both electrostatic and hydrophobic in nature. Subtraction of the spectrum of p25-MSL in buffer from the spectra in Figure 4 removes the mobile component (≤1% of the total spectral intensity) from these spectra, showing that this small mobile component represents unbound p25-MSL.

CW Saturation ESR Spectroscopy of Spin-Labeled Presequence. The dependences on microwave power of the ESR spectra from spin-labeled p25 presequence bound to DOPG membranes, both in the presence and in the absence of oxygen, are given in Figure 5. The saturation curves for the double-integrated intensity of the spectra given in Figure 5, together with the corresponding one for the sample in 10 mM chromium oxalate, are given in Figure 6. At higher microwave powers, the degree of saturation of the spin-label

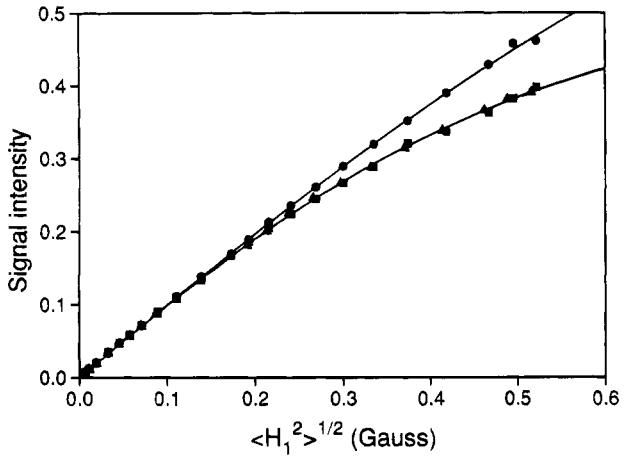

FIGURE 6: Dependence of the double-integrated intensity of the ESR spectra recorded at 30 °C, from p25-MSL bound to DOPG membranes in the absence (■) and in the presence of oxygen (●), and in the presence (▲) of argonated 10 mM CROX on the root mean square microwave magnetic field, $\langle H_1^2 \rangle^{1/2}$. The signal intensities are normalized relative to the number of spin labels in the samples (arbitrary units). The solid lines show the results of nonlinear least-squares fits to the saturation curves according to Snel and Marsh (1993), with rms errors of 2.7×10^{-3} (■), 2.6×10^{-3} (●), and 1.5×10^{-3} (▲).

attached to p25 that is evident in the absence of oxygen is reduced in the presence of oxygen. This is in contrast to the situation with CROX, which has hardly any effect on the saturation behavior of the spin-labeled peptide. Quantitative relaxation enhancements were obtained by the method described in Snel and Marsh (1993). The resulting accessibility parameter is the difference in the rate of the nitroxide relaxation in the presence and in the absence of paramagnetic species and hence provides a measure for the accessibility of the nitroxide spin label to the paramagnetic relaxation agent. Accessibility parameters to oxygen and to CROX are given for spin-labeled p25 bound to the different negatively charged lipid membranes in Table 2.

To calibrate the accessibility parameters obtained for the spin-labeled p25, comparable experiments were performed with spin-labeled phospholipids. The relative concentration of spin-labeled peptide was higher than that used for the spin-labeled lipids, but spin−spin interactions did not contribute measurably to the saturation properties of the spin-labeled peptide in the range of lipid/peptide ratios used. The effective T_1T_2 relaxation time products obtained from saturation measurements were 1.3 and 1.2×10^{-14} s^2 for p25-MSL in DOPG at L/P = 10 and 32 mol/mol, respectively, at 30 °C in the absence of oxygen. This suggests that the peptide is not aggregated appreciably at these concentrations and therefore that measurements on the spin-labeled lipids are appropriate for calibrating the location of the spin label on the peptide. The accessibility parameters for a lipid headgroup spin-label (T-PASL) and for lipids spin-labeled in the chain (5- and 14-PGSL), determined with and without p25-NEM bound to the different (mixed) lipid membranes, are given in Table 2. The accessibility of the phospholipid spin labels to oxygen is modified differentially by the bound p25-NEM. For the DOPG-containing membranes, the reduction in accessibility by binding of p25 is greatest at the 14-position in the acyl chain, whereas the accessibilities of the lipid spin-labels in the CL-containing membranes are hardly affected by binding of p25. The accessibility parameters obtained for the spin-labeled lipids in the presence of p25-NEM are those appropriate for interpreting the data with the spin-labeled p25 presequence. Specifically, these accessibility parameters contain the correction for any alteration in the lipid packing of the membrane, and thus for any changes in the membrane concentration of oxygen, that is caused by the binding of p25. Similar calibrations with phospholipid spin labels in the presence of p25-NEM are not performed for chromium oxalate because its action is limited to the aqueous phase (Snel & Marsh, 1993).

The accessibility parameters to oxygen for p25-MSL locate the label group on the peptide at a position between the 5-PGSL and 14-PGSL spin labels when bound to DOPG, at the position of the 14-PGSL spin-label when bound to DOPG/DOPC, at a position between the T-PASL and

Table 2: Accessibility Parameters to Oxygen and to Chromium Oxalate (CROX) for the Spin-Labeled p25 Presequence (p25-MSL) Bound to Different DOPG- or CL-Containing Bilayers and for Phospholipids Spin-Labeled at the 14- or 5-Position in the Acyl Chain or in the Headgroup (14-PGSL, 5-PGSL, and T-PASL, Respectively) Incorporated in DOPG- or CL-Containing Bilayers in the Absence (Lipid Alone) and in the Presence of Presequence Alkylated with NEM (p25-NEM) at the Indicated Lipid to Peptide Ratios (L/P)

		accessibility parameter[b] (10^{13} s^{-2} Gauss^{-1})				
				oxygen		
sample[a]	L/P (mol/mol)	oxygen	CROX	14-PGSL	5-PGSL	T-PASL
DOPG						
+ p25-MSL	32	7.6	0.06			
lipid alone				9.9	6.6	2.9
+ p25-NEM	27			7.6	7.5	3.7
DOPG/DOPC = 1:4 mol/mol						
+ p25-MSL	26	6.9	1.2			
lipid alone				12.3	7.7	2.7
+ p25-NEM	25			7.0	5.0	3.8
CL						
+ p25-MSL	24	4.6	0.5			
lipid alone				14.0	8.9	4.0
+ p25-NEM	21			15.0	6.8	3.0
CL/DOPC = 1:4 mol/mol						
+ p25-MSL	33	9.2	1.0			
lipid alone				15.0	8.8	2.9
+ p25-NEM	27			15.7	9.6	3.2

[a] The chromium oxalate concentration in the samples is 10 mM, and they are argonated. For the experiments in the presence of molecular oxygen, the samples are saturated with pure oxygen. Sample temperature is 30 °C. [b] Standard deviations in typical determinations of the accessibility parameter are in the region of 10−20%.

5-PGSL spin-labels when bound to CL, and at the position of the 5-PGSL spin-label when bound to CL/DOPC. It will be noted that several of the accessibilities of the spin label on the peptide to oxygen are equal to the maximum values recorded with the lipid spin labels. This indicates that the spin label on the peptide is fully accessible to oxygen under these circumstances and hence that the peptide is not aggregated appreciably, further supporting the appropriateness of the calibration using lipid spin labels. The low accessibilities to chromium oxalate indicate also that the spin label on p25-MSL is not located in the aqueous phase remote from the membrane surface, for which the accessibilities would be expected to be much higher (Snel & Marsh, 1993). The values obtained are comparable to, or slightly larger than, those obtained for the headgroup or 4-C atom position in phosphatidylcholine bilayers with 1 mM CROX (Snel & Marsh, 1993). Because the present experiments were conducted with 10 mM CROX, the accessibilities obtained with lipid mixtures containing 80% phosphatidylcholine (for which electrostatic effects are likely to be relatively small with the basic peptide bound) are consistent with the accessibility found for oxygen, i.e., with the spin label being buried deeper in the membrane than the 4-C atom position. A positive control for relaxation enhancement with 1 mM CROX is afforded by experiments with apocytochrome *c* (Snel et al., 1994b).

DISCUSSION

The mode of interaction of the presequence of yeast cytochrome oxidase subunit IV with bilayer membranes containing negatively charged lipids has been studied by three different approaches that utilize ESR spectroscopy. First, the perturbation of the lipid mobility on binding the presequence was studied with phospholipids spin-labeled in the *sn*-2 chain. These experiments were conducted at low lipid/peptide ratio in order to maximize interaction with the lipid. Second, the effects of membrane binding on the mobility of the peptide were studied via a spin label attached to cysteine-19 of the presequence. These experiments were conducted at a higher lipid/peptide ratio in order to minimize spin−spin interactions. Third, the location in the membrane of the section of the bound presequence around residue-19 was determined from the accessibility to paramagnetic relaxation agents. In the following, these three different aspects will be discussed in order, with reference to the lipid composition and a possible specific role for the unique mitochondrial phospholipid cardiolipin. A tentative model, within the framework of which the current results may be interpreted, is presented at the end of the Discussion.

Effects of the Presequence on Lipid Mobility. The binding of the p25 presequence to bilayers containing anionic lipids causes a large reduction in mobility of the lipid chains labeled either at the 5- or the 14-positions (Figures 1C and 3). The extent of chain immobilization is comparable to or greater than that induced either by the myelin basic protein (Sankaram et al., 1989) or by apocytochrome *c* (Görrissen et al., 1986), both of which are known to penetrate the membrane partially. This effect is considerably greater than that induced by cytochrome *c* which is known to be associated peripherally at the membrane surface (Görrissen et al., 1986). The abolition of the chain-melting phase transition of DMPG bilayers at high levels of binding of p25 (Figure 2A) also indicates that the presequence inserts between the lipid chains, hence disrupting their cooperative interactions. A similar effect on the lipid phase transition is also observed on binding of the myelin basic protein or apocytochrome *c*, but not of cytochrome *c*.

The induction by the presequence of a lipid population that is specifically restricted in its chain mobility, as is evidenced by the ESR spectra of the 14-PGSL spin label (Figure 3), is of particular significance. This immobilization extends to bilayers with contents of negatively charged lipids that approximate that of the physiological target membrane. It resembles superficially that of the lipid chains in contact with the intramembranous surface of integral proteins (Marsh, 1985), although the extent of motional restriction is appreciably smaller. Again, the effect is more similar to that observed on bilayer association of the myelin basic protein (Sankaram et al., 1989) or of apocytochrome *c* (Görrissen et al., 1986). The effective number of lipids per monomer whose chains are in direct contact with the bound presequence is relatively small. From Table 1, the number of motionally restricted lipids is approximately 2−3 for p25 bound to DOPG and approximately 1−2 for binding to cardiolipin. This suggests either that the p25 peptides are aggregated in the membrane or that the degree of membrane penetration is only partial. Evidence for aggregation of the peptide was obtained from the spin−spin broadening of the spectra of the spin-labeled peptide when it was present at concentrations comparable to that of the NEM-labeled peptide in the experiments with the spin-labeled lipids (L/P = 5 mol/mol; data not shown). Also, the experiments with the spin-labeled lipids indicate that the extent of lipid−peptide interaction is different in the two lipids and therefore the mode of association of the presequence with cardiolipin differs from that with DOPG. The likely reason for this difference is that the different mode of interaction and insertion results in a different aggregation state of the peptide, which extends also to the temperature dependence of the lipid−peptide interaction (cf. Table 1).

Effects of Binding on the Mobility of the Spin-Labeled Presequence. The spin-labeled presequence evidences a high degree of immobilization on binding to negatively charged bilayers, indicating an intimate association of the spin-labeled peptide segment with the lipids. The degree of peptide immobilization has been assessed additionally by saturation transfer ESR spectroscopy (data not shown) and found to correspond to rotational correlation times in the region of 10^{-7} s at 4 °C, whereas the conventional ESR spectra indicate correlation times of $\leq 10^{-8}$ s at 30 °C. These values are not characteristic of the rotational diffusion of large aggregates. The most likely origin for the reduction in mobility relative to the peptide free in solution is penetration into the bilayer, possibly coupled with a change in secondary structure, as proposed previously for spin-labeled apocytochrome *c* (Snel et al., 1994a). In support of this, it is found that the ESR spectra of the spin-labeled presequence are sensitive to the lipid phase transition (Figure 2B), which suggests also a penetration into the lipid chain region. There is little difference in the degree of immobilization of the spin-labeled presequence in the different lipid systems, suggesting that the interaction is both electrostatic and hydrophobic in nature. Although the degree of immobilization suggests penetration of the peptide into both DOPG and cardiolipin bilayers, the modes or extents of penetration may differ, corresponding to varying relative contributions from the electrostatic and

hydrophobic components of the interaction.

Membrane Location of the Spin-Labeled Presequence. The spin label on cysteine-19 of p25-MSL is located at the centre of the C-terminal half of the peptide. This is outside the section of the presequence that was found by NMR to have α-helical structure when bound to zwitterionic detergent micelles (Endo et al., 1989). It corresponds to a region that did not assume a regular secondary structure on association with the micelles. The evidence for the location in the membrane of the spin-labeled section of the presequence comes mostly from measurements of the accessibility to paramagnetic molecular oxygen. For p25-MSL bound to DOPG (L/P = 32 mol/mol), this corresponds to the region between the 5- and 14-positions of the lipid chain, and to the 14-position of the chain when bound to DOPG/DOPC at a mole ratio of 1:4 (L/P = 26 mol/mol) (see Table 2). These results give clear evidence for penetration of this section of p25 into the lipid bilayer. This conclusion is in agreement with those drawn above, both from the effects of the whole presequence on the mobility of the 14-PGSL spin-label and from the effects of binding to lipid on the mobility of the spin-labeled presequence.

For p25-MSL bound to cardiolipin (L/P = 24 mol/mol), the spin-labeled section of the presequence is located in the lipid headgroup region and in the region of the 5-position of the lipid chain when bound to CL/DOPC at a mole ratio of 1:4 (L/P = 33 mol/mol) (see Table 2). The results on the effect of the whole presequence on the mobility of the 14-PGSL label at high peptide/lipid ratio indicate direct contact with fewer lipid chain termini than in DOPG (Table 1). The experiments with paramagnetic relaxation agents agree with those on the mobility of the 14-PGSL label that the mode of association of the cytochrome oxidase subunit IV presequence with cardiolipin differs significantly from that with DOPG.

Comparison with Other Work and Functional Implications. All the ESR results presented above provide evidence for penetration of the p25 presequence into bilayers containing negatively charged phospholipids. They also indicate that the mode of association with cardiolipin, the tetraacylphospholipid unique to mitochondria, differs rather significantly from that with phosphatidylglycerol.

The subunit IV presequence has both positively charged and hydrophobic residues distributed throughout its length at positions that would favor the formation of an amphipathic α-helix. Indeed, ca. 50% helical structure is induced in the presequence on binding to phosphatidylglycerol, cardiolipin, their admixtures with 70 mol % phosphatidylcholine and to phospholipids that were extracted from mitochondria (Tamm & Bartoldus, 1990). The region from residue 3 to residue 11 has been shown to be in an α-helical conformation when associated with zwitterionic detergent micelles (Endo et al., 1989). The peptide conformation when bound to micelles may differ somewhat from that when bound to lipid vesicles but is broadly in agreement with the circular dichroism results quoted above.

Previous studies with lipid monolayers have indicated differences between the association with cardiolipin and with phosphatidylglycerol (Tamm, 1986; Török et al., 1994). The molecular area occupied by the presequence was found to be substantially smaller in cardiolipin monolayers (330 Å^2) than in phosphatidylglycerol monolayers (560 Å^2). The molecular area in phosphatidylglycerol monolayers is reasonably consistent with the size of a 25-residue amphipathic α-helix oriented with its axis parallel to the surface (Tamm, 1986). In contrast, polarized ATR studies have indicated that in partially rehydrated cardiolipin multibilayers the α-helical section of the presequence assumes a transmembrane orientation (Goormaghtigh et al., 1989). This different orientation is consistent with a reduction in the molecular area in cardiolipin monolayers, although a larger decrease might be expected, depending possibly on the surface pressure and the contribution from the nonhelical section of the peptide. Also the conditions, particularly the extent of hydration, differ in the two experiments.

As discussed above, a different mode of incorporation of the presequence in cardiolipin bilayers from that in phosphatidylglycerol bilayers is indicated both by the ESR spectra of the 14-PGSL lipid label and by the paramagnetic relaxation enhancements of the spin-labeled peptide by molecular oxygen. The varying extents of direct interaction with the lipid chains that are indicated by the former are consistent with the two orientations of the peptide that are described in the previous paragraph giving rise to different degrees of aggregation of the N-terminal section of the presequence at high peptide/lipid ratios. The differences in location within the membrane of the spin-labeled section of the presequence that are deduced from the ESR relaxation studies here refer to a different region of the peptide from that in which the α-helical structure is induced. Therefore, they provide evidence for additional differences in the interaction of the presequence with the two anionic lipids. It is likely that these are linked to the different forms of membrane integration of the α-helical section.

A specific, presequence-mediated affinity of mitochondrial precursor proteins for liposomes containing cardiolipin has been demonstrated (Ou et al., 1988). This affinity was proposed to be due to the unique structure of cardiolipin because the mitochondrial precursor proteins did not bind to liposomes containing other negatively charged phospholipids or to cardiolipin analogues. Recently, it has been shown in model systems that cardiolipin specifically is involved in the presequence-mediated formation of intermembrane contacts (Török et al., 1994). The presequence was found to promote efficient contact formation between lipid monolayers and large unilamellar vesicles that contained cardiolipin, but not between those containing phosphatidylglycerol. Further, the presequence has been found also to induce aggregation of large unilamellar vesicles that contain cardiolipin but not of those containing phosphatidylglycerol or several other anionic lipids (Leenhouts et al., 1993). The functional significance of cardiolipin in this membrane contact formation was emphasized by the fact that only in the presence of this mitochondrial lipid could the formation be reversed almost fully by the application of a transmembrane potential. Aggregation was observed also in the present experiments, suggesting the formation of interlamellar contacts, which from the ESR results must also be accompanied with membrane penetration by the peptide. Deletion of the C-terminal part of the presequence impairs the ability to form membrane contacts (Leenhouts et al., 1994).

The combined observations could be explained in terms of a model in which the N-terminal part of the presequence adopts an α-helical conformation upon interaction with the negatively charged membrane. In PG-containing membranes, the N-terminal helix is proposed to insert into the

bilayer in a configuration that is approximately parallel to the membrane surface (cf. Tamm, 1986). The spin label on cysteine-19 is localized rather deep in the membrane, between the 5-C atom and the 14-C atom of the lipid acyl chains. Because it is inserted deeply, the formation of intermembrane contacts is more difficult and experimentally is not observed. In CL-containing membranes, the N-terminal α-helix may insert parallel to the acyl chains in the lipid bilayer (cf. Goormaghtigh et al., 1989). The spin label on cysteine-19 in the C-terminal part of the presequence is localized between the headgroup region and the 5-C atom of the lipid acyl chain. The rest of the C-terminal part of p25 containing positive charges could then be localized more superficially and be involved in the intermembrane contacts. It can be speculated therefore that the location of the presequence, spin-labeled at position 19, closer to the surface of cardiolipin-containing membranes that is found in the present work may facilitate the formation of intermembrane contacts and their reversal by the transmembrane potential.

ACKNOWLEDGMENT

We thank Prof. H. M. McConnell for the opportunity to synthesize and purify p25 in his laboratory and Prof. B. de Kruijff for critically reading the manuscript and for the use of the HPLC equipment during the labeling of p25.

REFERENCES

Bailar, J. C., Jr., & Jones, E. M. (1939) *Inorg. Syn. 1*, 35−38.
Comfurius, P., & Zwaal, R. F. A. (1977) *Biochim. Biophys. Acta 488*, 36−42.
Daum, G. (1985) *Biochim. Biophys. Acta 822*, 1−42.
De Kroon, A. I. P. M., De Gier, J., & De Kruijff, B. (1991) *Biochim. Biophys. Acta 1068*, 111−124.
De Kroon, A. I. P. M., & McConnell, H. M. (1994) *J. Immunol. 152*, 609−619.
Eibl, H. (1978) *Proc. Natl. Acad. Sci. U.S.A. 75*, 4074−4077.
Endo, T., Shimada, I., Roise, D., & Inagaki, F. (1989) *J. Biochem. (Tokyo) 106*, 396−400.
Esmann, M., Hankovszky, H. O., Hideg, K., & Marsh, D. (1989) *Biochim. Biophys. Acta 978*, 209−215.
Fajer, P., & Marsh, D. (1982) *J. Magn. Reson. 49*, 212−224.
Frey, S., & Tamm, L. K. (1990) *Biochem. J. 272*, 713−719.
Goormaghtigh, E., Martin, I., Vandenbranden, M., Brasseur, R., & Ruysschaert, J. M. (1989) *Biochem. Biophys. Res. Commun. 158*, 610−616.
Görrissen, H., Marsh, D., Rietveld, A., & De Kruijff, B. (1986) *Biochemistry 25*, 2904−2910.
Horváth, L. I., Brophy, P. J., & Marsh, D. (1988) *Biochemistry 27*, 46−52.
Kiebler, M., Becker, K., Pfanner, N., & Neupert, W. (1993) *J. Membr. Biol. 135*, 191−207.
Leenhouts, J. M., De Gier, J., & De Kruijff, B. (1993) *FEBS Lett. 327*, 172−176.
Leenhouts, J. M., Török, Z., Demel, R. A., De Gier, J., & De Kruijff, B. (1994) *Mol. Membr. Biol. 11*, 159−164.
Maduke, M., & Roise, D. (1993) *Science 260*, 364−367.
Malati, M. A., & Abdul Azim, A. A. (1959) *Egypt. J. Chem. 2*, 47.
Malati, M. A., & Abdul Azim, A. A. (1960) *Chem. Abstr. 54*, 2085f.
Marsh, D. (1982) *Tech. Life Sci.: Biochem. B4/II*, B426/1−44.
Marsh, D. (1985) in *Progress in Protein−Lipid Interactions* (Watts, A., & De Pont, J. J. H. H. M., Eds.) Vol. 1, pp 143−172, Elsevier, Amsterdam.
Marsh, D., & Watts, A. (1982) in *Lipid−Protein Interactions* (Jost, P. C., & Griffith, O. H., Eds.) Vol. 2, pp 53−126, Wiley-Interscience, New York.
Ou, W. J., Ito, A., Umeda, M., Inoue, K., & Omura, T. (1988) *J. Biochem. (Tokyo) 103*, 589−595.
Roise, D. (1992) *Proc. Natl. Acad. Sci. U.S.A. 89*, 608−612.
Roise, D., Horvath, S. J., Tomich, J. M., Richards, J. H., & Schatz, G. (1986) *EMBO J. 5*, 1327−1334.
Rouser, G., Fleischer, S., & Yamamoto, A. (1970) *Lipids 5*, 494−496.
Sankaram, M. B., Brophy, P. J., & Marsh, D. (1989) *Biochemistry 28*, 9685−9691.
Snel, M. M. E., & Marsh, D. (1993) *Biochim. Biophys. Acta 1150*, 155−161.
Snel, M. M. E., De Kruijff, B., & Marsh, D. (1994a) *Biochemistry 33*, 7146−7156.
Snel, M. M. E., De Kruijff, B., & Marsh, D. (1994b) *Biochemistry 33*, 11150−11157.
Tamm, L. K. (1986) *Biochemistry 25*, 7470−7476.
Tamm, L. K. (1991) *Biochim. Biophys. Acta 1071*, 123−148.
Tamm, L. K., & Bartoldus, I. (1990) *FEBS Lett. 272*, 29−33.
Török, Z., Demel, R. A., Leenhouts, J. M., & De Kruijff, B. (1994) *Biochemistry 33*, 5589−5594.
Van Dijck, P. W. M., De Kruijff, B., Verkleij, A. J., Van Deenen, L. L. M., & De Gier, J. (1978) *Biochim. Biophys. Acta 512*, 84.
Von Heijne, G. (1986) *EMBO J. 5*, 1335−1342.
Watts, A., Harlos, K., Maschke, W., & Marsh, D. (1978) *Biochim. Biophys. Acta 510*, 63−74.

BI9421174